ELSEVIER

Journal of Organometallic Chemistry 565 (1998) 11–18

Journal of Organometallic Chemistry

The unusual attachment of an alkyne across the open edge of a Rh_2Pd complex[1]

Geoffrey R. County, Ron S. Dickson *, Gary D. Fallon

Department of Chemistry, Monash University, Clayton, Victoria 3168, Australia

Received 1 November 1997

Abstract

A structurally interesting hetero-trinuclear complex of formula $(\eta^5\text{-}C_5H_5)_2Rh_2Pd(\mu_3\text{-}CO)(\mu\text{-}\eta^1\text{:}\eta^2\text{:}\eta^2\text{-}CF_3C_2CF_3)\{\eta^2\text{-}Ph_2P(CH_2)_2PPh_2\}$ (**III**) has been formed from the reaction between $(\eta^5\text{-}C_5H_5)_2Rh_2(CO)(\mu\text{-}\eta^1\text{:}\eta^1\text{-}CF_3C_2CF_3)\{\eta^1\text{-}Ph_2P(CH_2)_2PPh_2\}$(**II**) and $(\eta^5\text{-}C_5H_5)Pd(\eta_3\text{-}C_3H_5)$. Determination of the structure of (**III**) by X-ray crystallography has shown that there is an open Rh_2Pd core with an unusual attachment of the alkyne. This is σ-bonded to the central rhodium and sits across the open Rh···Pd edge of the core. Molecular modeling established that one CF_3 is free to rotate but the other is restrained. The bisphosphine, which was initially attached to rhodium, is chelated to palladium. In solution, a second isomer (**IV**) coexists with (**III**); spectroscopic results indicate that (**IV**) incorporates a $\overline{Rh\text{–}C(O)\text{–}C(CF3)=}CCF_3$ unit within a structure that has a closed Rh_2Pd core. Variable temperature NMR data indicate that the molecular structures of both isomers are fluxional in solution.

Keywords: Rhodium; Palladium; Heteronuclear cluster; Alkyne

1. Introduction

There is considerable interest in the structures and chemical behavior of molecular complexes containing a core of different metals [1,2]. Although the range of heteronuclear complexes incorporating M–M′ bonds is extensive, there are still relatively few complexes containing Rh–Pt or Rh–Pd bonds. Recently, we described some interesting structural features of a hetero-trinuclear complex $(\eta^5\text{-}C_5H_5)_2Rh_2Pt(\mu_3\text{-}CO)(\mu_2\text{-}\eta^1\text{:}\eta^1\text{:}\eta^2\text{-}CF_3C_2CF_3)(COD)$ [3]. In the solid state, there is a V-shaped arrangement of the metals with one Rh–Rh and only one Rh–Pt bond; the alkyne is σ-attached to Pt and one Rh and π-bonded to the remaining Rh. In solution, however, two isomers co-exist. The static solid state structure is retained in one, but the other has a closed Rh_2Pt core and the alkyne rotates freely on this face at room temperature (r.t.). Interconversion between the two isomers involves facile Rh–Pt bond making and breaking at r.t. We have now discovered a Rh_2Pd system with different but equally fascinating structural features, and we describe the formation, structure, and molecular dynamics of this complex in the present paper.

2. Experimental

2.1. General procedures

Reactions were carried out under an atmosphere of purified nitrogen in oven-dried Schlenk flasks. Purification of the product was achieved by preparative-scale TLC, which was carried out on 20 × 20 cm glass plates with a 1:1 silica gel G-HF_{254} mixture (Type 60, Merck) as adsorbent. Separation was achieved on deactivated

* Corresponding author.

[1] Our best wishes to Michael Bruce on the occasion of his 60th birthday.

0022-328X/98/$19.00
PII S0022-328X(98)00494-X

plates, obtained by drying at r.t. only. Microanalysis was performed by the Campbell Microanalytical Laboratory, University of Otago, New Zealand.

2.2. Instrumentation

Solution IR spectra (KBr windows) were obtained using a Perkin Elmer 1600 Fourier transform spectrometer. NMR spectra were measured on Bruker AC 200 or AM 300 spectrometers. The ^{1}H-NMR spectra were measured at 200 or 300 MHz, ^{19}F at 282.4 MHz, ^{13}C at 50.3 or 75 MHz, and ^{31}P{^{1}H} at 121.5 MHz; deuterated solvents ($CDCl_3$, acetone-d_6, toluene-d_8) were used as internal locks. Chemical shifts are in parts per million from internal Me_4Si for ^{1}H and ^{13}C, from CCl_3F for ^{19}F, and from (external) 85% H_3PO_4 for ^{31}P{^{1}H}; in all cases, a positive chemical shift denotes a resonance downfield from the reference. A Silicon Graphics Indy computer equipped with the Insight II software package [4] was used for molecular modeling.

2.3. Materials

Acetone was analytical grade reagent; hydrocarbons and dichloromethane were purified by distillation under nitrogen from the appropriate drying agent [5]. All solvents were stored in the dark over activated 4A molecular sieves and were purged with nitrogen prior to use. The dirhodium complex $(\eta^5\text{-}C_5H_5)_2Rh_2(\mu\text{-}CO)(\mu\text{-}\eta^2{:}\eta^2\text{-}CF_3C_2CF_3)$ (**I**) was prepared as described by Dickson et al. [6], and converted to $(\eta^5\text{-}C_5H_5)_2Rh_2(CO)(\mu\text{-}\eta^1{:}\eta^1\text{-}CF_3C_2CF_3)\{\eta^1\text{-}Ph_2P(CH_2)_2PPh_2\}$(**II**) by treatment with bis(diphenylphosphino)ethane [7]. The palladium complex $(\eta^5\text{-}C_5H_5)Pd(\eta^3\text{-}C_3H_5)$ was prepared according to ref. [8].

2.4. Reaction of $(\eta^5\text{-}C_5H_5)_2Rh_2(CO)(\mu\text{-}\eta^1{:}\eta^1\text{-}CF_3C_2CF_3)\{\eta^1\text{-}Ph_2P(CH_2)_2PPh_2\}$ (II) with $(\eta^5\text{-}C_5H_5)Pd(\eta^3\text{-}C_3H_5)$

A slight excess of the palladium complex $(\eta^5\text{-}C_5H_5)Pd(\eta^3\text{-}C_3H_5)$ (0.043 g, 0.20 mmol) was added to a solution of $(\eta^5\text{-}C_5H_5)_2Rh_2(CO)(\mu\text{-}\eta^1{:}\eta^1\text{-}CF_3C_2CF_3)\{\eta^1\text{-}Ph_2P(CH_2)_2PPh_2\}$(**II**) (0.120 g, 0.13 mmol) in acetone (30 ml). The solution was stirred and monitored periodically to determine when all of (**II**) had been consumed; this took 48 h. Most of the solvent was removed under reduced pressure, and the remaining solution was purified by TLC with a 1:1 mixture of petroleum spirit and diethyl ether as eluent. Only one major band developed, and this was extracted with dichloromethane. Evaporation of solvent left a dark brown–orange solid which was identified as partially solvated $(\eta^5\text{-}C_5H_5)_2Rh_2Pd(\mu_3\text{-}CO)(\mu\text{-}\eta^1{:}\eta^2{:}\eta^2\text{-}CF_3C_2CF_3)\{\eta^2\text{-}Ph_2P(CH_2)_2PPh_2\}$ (**III**) (0.020 g, 21%). Anal. Found: C 46.3, H 3.2%. For $C_{41}H_{34}F_6OP_2PdRh_2$. Calc.: C 47.7, H 3.3%. For the dichloromethane solvate $C_{42}H_{36}Cl_2F_6OP_2PdRh_2$ Calc.: C 45.1, H 3.2%. IR spectrum (KBr disk): ν(CO) 1737 m cm^{-1}. Spectroscopic data indicated that in solution (**III**) co-existed with another isomer $(\eta^5\text{-}C_5H_5)_2Rh_2Pd\{\mu\text{-}\eta^1{:}\eta^2{:}\eta^2\text{-}C(O)C(CF_3)C(CF_3)\}\{\eta^2\text{-}Ph_2P(CH_2)_2PPh_2\}$ (**IV**). IR (CH_2Cl_2) cm^{-1}: ν(CO) 1746 m; (toluene): ν(CO) 1754 m, 1707 w . NMR spectral data: see Table 1.

2.5. Crystallography of $(\eta^5\text{-}C_5H_5)_2Rh_2Pd(\mu_3\text{-}CO)(\mu\text{-}\eta^1{:}\eta^2{:}\eta^2\text{-}CF_3C_2CF_3)\{\eta^2\text{-}Ph_2P(CH_2)_2PPh_2\}$ (III)

Dark orange–brown crystals of $(\eta^5\text{-}C_5H_5)_2Rh_2Pd(\mu_3\text{-}CO)(\mu\text{-}\eta^1{:}\eta^2{:}\eta^2\text{-}CF_3C_2CF_3)\{\eta^2\text{-}Ph_2P(CH_2)_2PPh_2\}$ (**III**) solvated with dichloromethane were grown by slow diffusion of hexane into a saturated solution of the complex in dichloromethane. A summary of the crystal data is given in Table 2. Selected bond lengths and angles are presented in Tables 3 and 4, while H atom coordinates and isotropic displacement coefficients are shown in Table 5.

3. Results and discussion

We have prepared a number of hetero-polynuclear complexes based on the addition of complexes with labile ligands to the highly reactive dirhodium complex $(\eta^5\text{-}C_5H_5)_2Rh_2(\mu\text{-}CO)(\mu\text{-}\eta^2{:}\eta^2\text{-}CF_3C_2CF_3)$ (**I**). As an example, the previously mentioned complex $(\eta^5\text{-}C_5H_5)_2Rh_2Pt(\mu_3\text{-}CO)(\mu_2\text{-}\eta^1{:}\eta^1{:}\eta^2\text{-}CF_3C_2CF_3)(COD)$ was formed from (**I**) and $Pt(COD)_2$ [3]. Bridge-assisted reactions provide another route to the formation of hetero-polynuclear complexes. Recently, we applied this approach to the formation of some complexes containing the $Rh\{\mu\text{-}\eta^1{:}\eta^1\text{-}Ph_2P(CH_2)_nPPh_2\}M$ link [10]. An example was the formation of $(\eta^5\text{-}C_5H_5)_2Rh_2(CO)(\mu\text{-}\eta^1{:}\eta^1\text{-}CF_3C_2CF_3)\{\mu\text{-}\eta^1{:}\eta^1\text{-}Ph_2P(CH_2)_2PPh_2\}Cr(CO)_5$ from the reaction between $(\eta^5\text{-}C_5H_5)_2Rh_2(CO)(\mu\text{-}\eta^1{:}\eta^1\text{-}CF_3C_2CF_3)\{\eta^1\text{-}Ph_2P(CH_2)_2PPh_2\}$ and $Cr(CO)_5\cdot THF$.

3.1. Formation of the complex $(\eta^5\text{-}C_5H_5)_2Rh_2Pd(\mu_3\text{-}CO)(\mu\text{-}\eta^1{:}\eta^2{:}\eta^2\text{-}CF_3C_2CF_3)\{\eta^2\text{-}Ph_2P(CH_2)_2PPh_2\}$

The palladium complex $(\eta^5\text{-}C_5H_5)Pd(\eta^3\text{-}C_3H_5)$, which was first prepared by Shaw [11], is a useful source of palladium (0) complexes because both hydrocarbon ligands are labile [12,13]. It has been used, for example, in the formation of $Pd(PBu^t_3)_2$ [14]. To the best of our knowledge, it has not been involved previously in the synthesis of hetero-polynuclear complexes. When a slight excess of $(\eta^5\text{-}C_5H_5)Pd(\eta^3\text{-}C_3H_5)$ was added to an acetone solution of $(\eta^5\text{-}C_5H_5)_2Rh_2(CO)(\mu\text{-}\eta^1{:}\eta^1\text{-}CF_3C_2CF_3)\{\eta^1\text{-}Ph_2P(CH_2)_2PPh_2\}$(**II**), there was

Table 1
Some variable temperature ^{1}H- and ^{19}F-NMR data for the isomers $(\eta^5\text{-}C_5H_5)_2Rh_2Pd(\mu_3\text{-}CO)(\mu\text{-}\eta^1{:}\eta^2{:}\eta^2\text{-}CF_3C_2CF_3)\{\eta^2\text{-}Ph_2P(CH_2)_2PPh_2\}$ (**III**) and $(\eta^5\text{-}C_5H_5)_2Rh_2Pd\{\mu\text{-}\eta^1{:}\eta^2{:}\eta^2\text{-}C(O)C(CF_3)C(CF_3)\}\{\eta^2\text{-}Ph_2P(CH_2)_2PPh_2\}$ (**IV**)

Solvent	Isomer	Ratio[a]	^{1}H-NMR $\delta(C_5H_5)$ (fast exchange)	T_c (K)[b]	^{1}H-NMR $\delta(C_5H_5)$ (slow exchange)	^{19}F-NMR $\delta(CF_3)$ (fast exchange)	T_c (K)	^{19}F-NMR $\delta(CF_3)$ (slow exchange)
$CDCl_3$	(III)	12.4	5.01	225	5.30, 4.71	−50.9	233	−51.1, −51.6
	(IV)	1.0	4.72	267	4.87, 4.42	—	—	−49 5, −54.8
Acetone-d_6	(III)	2.5	5.05	230	5.35, 4.76	−49.1	—	[c]
	(IV)	1.0	4.81	270	5.05, 4.54	—	—	−47.8, −53.0
Toluene-d_8	(III)	3.6	5.10	230	5.55, 4.95	−48.7	240	−49.0, −49.4
	(IV)	1.0	4.81	268	4.96, 4.60	—	—	−47.8, −52.6

[a] Ratios were determined from the relative intensities of the C_5H_5 peaks in the ^{1}H-NMR spectra at 300 K. [b] T_c, coalescence temperature. [c] No clear separation of peaks.

some darkening of the initially red solution. The reaction was monitored by spot TLC until it was evident that no unchanged (**II**) remained. During the TLC monitoring, a yellow–brown spot appeared and its intensity increased over the period of the reaction. This was the only major product detected, and it was isolated as a dark brown, air sensitive solid by preparative TLC of the reaction mixture. It proved difficult to characterize the complex from elemental analyses and spectroscopic results, but the crystal and molecular structure was determined by X-ray crystallography. This established unequivocally that the formula is $(\eta^5\text{-}C_5H_5)_2Rh_2Pd(\mu_3\text{-}CO)(\mu\text{-}\eta^1{:}\eta^2{:}\eta^2\text{-}CF_3C_2CF_3)\{\eta^2\text{-}Ph_2P(CH_2)_2PPh_2\}$ (**III**). Although the IR and multinuclear NMR results support this formulation, they also indicate that a second isomer co-exists in solution.

Table 2
Summary of crystal structure data for the complex $(\eta^5\text{-}C_5H_5)_2Rh_2Pd(\mu_3\text{-}CO)(\mu\text{-}\eta^1{:}\eta^2{:}\eta^2\text{-}CF_3C_2CF_3)\{\eta^2\text{-}Ph_2P(CH_2)_2PPh_2\}\cdot CH_2Cl_2$ (III)

Crystal data	
Empirical formula	$C_{42}H_{36}Cl_2F_6OP_2PdRh_2$
Formula weight	1115.8
Crystal dimensions (mm^3)	$0.24\times0.29\times0.19$
Crystal system	Triclinic
Lattice type	Primitive
No. reflections for unit cell determination	31
2θ range (°)	5–27
Lattice parameters	
a (Å)	11.813(2)
b (Å)	13.527(3)
c (Å)	13.966(3)
α (°)	111.77(1)
β (°)	90.87(1)
γ (°)	99.43 (1)
Volume ($Å^3$)	2037.5(7)
Space group	$P\bar{1}$
Z	2
$D_{calc.}$ (g cm^{-3})	1.82
$F(000)$	1100
μ(Mo–K_α) (cm^{-1})	14.9
Intensity measurements	
Diffractometer	Nicolet R3m/V
Radiation	Mo–K_α ($\lambda=0.71073$ Å) graphite monochromated
Temperature (K)	293
Scan type	ω
Scan rate (° min^{-1})	2.39–10.19
Scan width (°)	0.7
$2\theta_{max}$ (°)	50
Index range	$-1\le h\le14$, $-16\le k\le16$, $-16\le l\le16$
Reflections collected	8336
Independent	7195 ($R_{int}=0$ 073)
Observed	6239 [$F>6.0\sigma(F)$]
Corrections	Lorentz-polarization, absorption (trans. factors: 0.794–0.649)
Structure solution and refinement	
Structure solution [9]	SHELXTL Plus
Refinement [9]	Full-matrix least-squares on F
Least-squares weights	$[\sigma^2(F)+0.0007F^2]^{-1}$
No variables	533
Residuals: R_1, wR_2 [$F>6.0\sigma(F)$]	0.023, 0.034
R indices (all data)	0.029, 0.037
GOF indicator	1.10
Largest difference peak and hole (e $Å^{-3}$)	0.65, −0.76

Table 3
Selected bond lengths (Å) for the complex $(\eta^5\text{-}C_5H_5)_2Rh_2Pd(\mu_3\text{-}CO)(\mu\text{-}\eta^1{:}\eta^2{:}\eta^2\text{-}CF_3C_2CF_3)\{\eta^2\text{-}Ph_2P(CH_2)_2PPh_2\}$ (III) (estimated S.D. in parentheses)

Metal–metal			
Rh(1)–Rh(2)	2.629(1)	Rh(1)–Pd	2.671(1)
Rh(2)···Pd	3.408(1)		
Hexafluorobut-2-yne			
Rh(1)–C(3)	2.039(3)	Pd–C(3)	2.609(3)
Rh(2)–C(3)	2.005(2)	Pd–C(4)	2.067(3)
Rh(2)–C(4)	2.142(3)	C(3)–C(4)	1.393(5)
Carbonyl ligand			
Rh(1)–C(1)	1.981(3)	Rh(2)–C(1)	2.004(3)
Pd–C(1)	2.594(3)	C(1)–O(1)	1.177(3)
Bis(diphenylphosphino)ethane			
Pd–P(1)	2.285(1)	Pd–P(2)	2.302(1)
P(1)–C(16)	1.854(3)	P(2)–C(17)	1.848(3)
P(1)–C(18)	1.824(3)	P(2)–C(30)	1.818(3)
P(1)–C(24)	1.822(3)	P(2)–C(36)	1.818(3)
Cyclopentadienyl rings			
C(6)–C(7)	1.410(5)	C(6)–C(10)	1.438(5)
C(7)–C(8)	1.416(4)	C(8)–C(9)	1.421(5)
C(9)–C(10)	1.411(4)	C(11)–C(12)	1.429(5)
C(11)–C(15)	1.407(7)	C(12)–C(13)	1.389(7)
C(13)–C(14)	1.415(5)	C(14)–C(15)	1.409(6)

3.2. The crystal and molecular structure of $(\eta^5\text{-}C_5H_5)_2Rh_2Pd(\mu_3\text{-}CO)(\mu\text{-}\eta^1{:}\eta^2{:}\eta^2\text{-}CF_3C_2CF_3)\{\eta^2\text{-}Ph_2P(CH_2)_2PPh_2\}$ (III)

A drawing of the molecular structure of the complex is shown in Fig. 1. A clearer representation of the bonding interactions is given in (**III**). The core of the structure shows a V-shaped arrangement of the metal atoms with M–M bonds between Rh(1)–Rh(2) and Rh(1)–Pd; the M–M distances are 2.629(1) and 2.671(1) Å, respectively. The Rh(2)···Pd distance of 3.408(1) Å is regarded as nonbonding. It is considerably longer than previously reported Rh–Pd bond lengths which fall within the range 2.594(1)–2.699(1) Å) [15–18]. The Rh(2)–Rh(1)–Pd angle is 80.0(10)°. The overall arrangement is similar to that for $(\eta^5\text{-}C_5H_5)_2Rh_2Pt(\mu_3\text{-}CO)(\mu_2\text{-}\eta^1{:}\eta^1{:}\eta^2\text{-}CF_3C_2CF_3)$(COD), where the corresponding bond parameters are Rh(1)–Rh(2) 2.641(1), Rh(1)–Pt 2.628(1), Rh(2)···Pd 3.361(4) Å and Rh(2)–Rh(1)–Pt 79.3° [3].

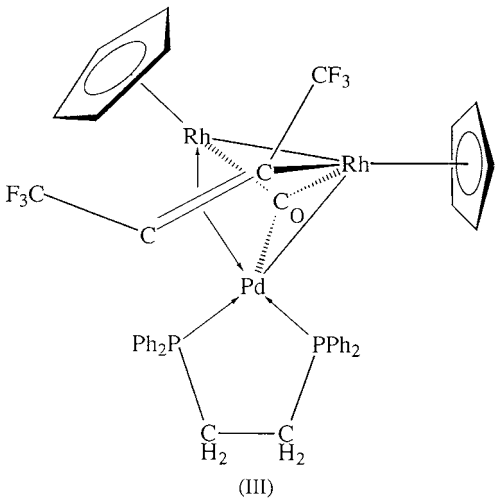

(III)

The most interesting feature of the structure is the location of the alkyne. The C(3)–C(4) bond axis of the ligand is approximately parallel to the plane defined by the metal atoms, with an angle of 27.0° between the lines Pd–Rh(1) and C(3)–C(4). The torsion angle Rh(1)–C(3)–C(4)–Pd is 35.5°. The positioning of the alkyne, and the Rh(1)–C(3) distance of 2.039(3) Å, indicate that Rh(1) is σ-bound to one end of the alkyne unit. The orientation of the alkyne coupled with the observed distances for Rh(2)–C(3) (2.005(2) Å) and Rh(2)–C(4) (2.142(3) Å) indicate that Rh(2) is π-attached to the alkyne. Based on the twist of the alkyne relative to the Rh(1)–Pd bond, we believe that the attachment of the alkyne to Pd is best described as asymmetric π-bonding; the Pd–C(3) distance (2.609(3) Å) is significantly longer than that for Pd–C(4) (2.067(3) Å). This μ_3-η^1:η^2:η^2-attachment of the alkyne to the metal core is, to the best of our knowledge, unprecedented. It differs significantly from the more common μ_3-η^1:η^1:η^2-attachment in the complex (η^5-C_5H_5)$_2$Rh$_2$Pt(μ_3-CO)(μ_2-η^1:η^1:η^2-$CF_3C_2CF_3$) (COD), where the alkyne is σ-attached to one Rh and Pt and lies parallel to the Rh–Pt bond.

The alkyne C(3)–C(4) distance of 1.393(5) Å and the average C–F distance of 1.345 Å are similar to previously reported bond lengths for hexafluorobut-2-

Table 4
Selected bond angles (°) for the complex (η^5-C_5H_5)$_2$Rh$_2$Pd(μ_3-CO)(μ-η^1:η^2:η^2-$CF_3C_2CF_3$){η^2-$Ph_2P(CH_2)_2PPh_2$} (III)

Around the metals			
Rh(2)–Rh(1)–Pd	80.0(1)	Rh(1)–Rh(2)–C(1)	48.4(1)
Pd–Rh(1)–C(1)	65.8(1)	Rh(1)–Rh(2)–C(3)	49.8(1)
Pd–Rh(1)–C(3)	65.7(1)	Rh(1)–Rh(2)–C(4)	73.2(1)
Rh(2)–Rh(1)–C(1)	49.1(1)	Rh(1)–Pd–C(4)	73.4(1)
Rh(2)–Rh(1)–C(3)	50.3(1)	P(1)–Pd–P(2)	85.7(1)
Carbonyl ligand			
Rh(1)–C(1)–Rh(2)	82.6(1)	Rh(1)–C(1)–O(1)	140.0(3)
Rh(1)–C(1)–Pd	70.0(1)	Rh(2)–C(1)–O(1)	135.9(2)
Rh(2)–C(1)–Pd	94.8(1)	Pd–C(1)–O(1)	109.0(2)
Bis(diphenylphosphino)ethane ligand			
Pd–P(1)–C(16)	108.2(1)	Pd–P(2)–C(17)	106.5(1)
Pd–P(1)–C(18)	121.2(1)	Pd–P(2)–C(30)	112.1(1)
Pd–P(1)–C(24)	113.5(1)	Pd–P(2)–C(36)	123.5(1)
C(16)–P(1)–C(18)	101.9(1)	C(17)–P(2)–C(30)	103.0(1)
C(16)–P(1)–C(24)	104.3(1)	C(17)–P(2)–C(36)	101.7(1)
C(18)–P(1)–C(24)	106.1(1)	C(30)–P(2)–C(36)	107.6(1)
Hexafluorobut-2-yne			
C(3)–Rh(2)–C(4)	38.7(1)	Rh(2)–C(4)–C(3)	67.3(2)
Rh(2)–C(3)–C(4)	74.0(1)	C(3)–C(4)–C(5)	127.2(2)
C(2)–C(3)–C(4)	124.7(3)	Rh(2)–C(4)–Pd	108.1(1)
Rh(1)–C(3)–C(4)	112.3(2)	Pd–C(4)–C(3)	96.0(2)
Pd–C(3)–C(4)	52.0(2)	Pd–C(4)–C(5)	124.8(2)
Cyclopentadienyl rings			
C(7)–C(6)–C(10)	108.8(3)	C(6)–C(7)–C(8)	107.0(3)
C(7)–C(8)–C(9)	109.2(3)	C(8)–C(9)–C(10)	107.6(3)
C(6)–C(10)–C(9)	107.4(3)	C(12)–C(11)–C(15)	108.4(4)
C(11)–C(12)–C(13)	107.8(4)	C(12)–C(13)–C(14)	107.9(4)
C(13)–C(14)–C(15)	108.9(4)	C(11)–C(15)–C(14)	106.9(3)

Table 5
Hydrogen atom coordinates ($\times 10^4$) and isotropic displacement coefficients (Å$^2 \times 10^3$)

	x	y	z	U
H(6A)	2588	5961	2711	80
H(7A)	448	5530	2136	80
H(8A)	169	4064	327	80
H(9A)	2134	3667	−261	80
H(10A)	3633	4802	1227	80
H(11A)	−968	700	2902	80
H(12A)	−1308	2581	4062	80
H(13A)	−1919	3487	2906	80
H(14A)	−1862	2229	1046	80
H(15A)	−1393	457	1033	80
H(16A)	5541	557	1612	80
H(16B)	5903	1801	2194	80
H(17A)	5806	1531	468	80
H(17B)	4606	779	264	80
H(19A)	5646	2893	3888	80
H(20A)	6371	3335	5590	80
H(21A)	5648	2249	6500	80
H(22A)	4244	712	5695	80
H(23A)	3539	243	3973	80
H(25A)	1722	214	1485	80
H(26A)	695	−1579	824	80
H(27A)	1565	−2980	912	80
H(28A)	3484	−2615	1596	80
H(29A)	4523	−835	2223	80
H(31A)	4715	4323	3001	80
H(32A)	6235	5695	3961	80
H(33A)	7960	5965	3211	80
H(34A)	8176	4856	1506	80
H(35A)	6673	3439	555	80
H(37A)	2986	1108	−701	80
H(38A)	2484	986	−2369	80
H(39A)	3211	2403	−2903	80
H(40A)	4494	3918	−1775	80
H(41A)	5057	4015	−126	80
H(42A)	386	9512	4480	80
H(42B)	1007	9147	3484	80
H(43A)	694	7658	3943	80
H(43B)	1471	8003	3169	80

yne in the complexes $(\eta^5\text{-}C_5H_5)_2(THD)Rh_3(\mu_3\text{-}CO)(\mu\text{-}\eta^1{:}\eta^1{:}\eta^2\text{-}CF_3C_2CF_3)$ (THD = 2,2,6,6-tetramethyl-3,5-heptanedionate) [19] and $(\eta^5\text{-}C_5H_5)_2Rh_2Ir(\mu\text{-}PPh_2)(CO)_2(\mu\text{-}\eta^1{:}\eta^1{:}\eta^2\text{-}CF_3C_2CF_3)$ [20].

The triply bridged carbonyl ligand is asymmetrically attached to the three metal atoms, with M–C distances of 1.981(3) for Rh(1)–C(1), 2.004(3) for Rh(2)–C(1) and 2.594(3) Å for Pd–C(1). All fall within the normal range for triply bridging carbonyls on rhodium [21,22] and palladium [23] clusters. The bis(diphenylphosphino)ethane ligand, which was initially unidentate attached to rhodium, is now chelated to palladium. Palladium–phosphorus distances of 2.285(1) and 2.302(1) Å are consistent with those for other palladium compounds containing this ligand [24,25].

3.3. Discussion of the orientation of the alkyne

In many trinuclear alkyne metal clusters, there is a correlation between the cluster electron count and the orientation of the alkyne [2]. In general, the $\mu_3\text{-}\eta^2(\perp)$ alkyne bonding mode is adopted in 46-electron clusters such as $Fe_3(CO)_9(RC_2R)$ [26,27] and $Fe_2Ru(CO)_9(RCR)$, whereas the $\mu_3\text{-}\eta^2(//)$ mode is observed in most 48-electron clusters including $Ru_3(CO)_9(RC_2R)(H)_2$ [28,29] and $Os_3(CO)_{10}(RC_2R)$ [29–31]. However, the established 'rules' can be broken [2]. In a recent paper [19], we demonstrated that the alkyne is aligned parallel to a Rh–Rh bond in the 46-electron cluster $(\eta^5\text{-}C_5H_5)_2(\eta^2\text{-}THD)Rh_3(\mu_3\text{-}CO)(\mu\text{-}\eta^1{:}\eta^1{:}\eta^2\text{-}CF_3C_2CF_3)$.

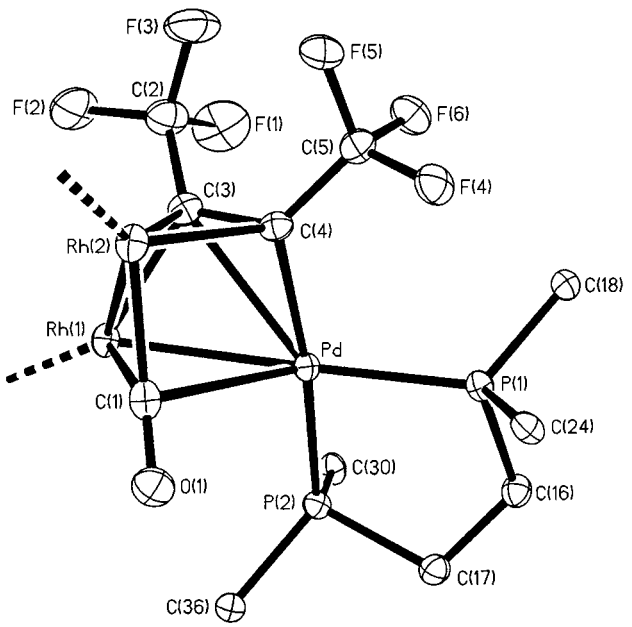

Fig. 1. The molecular structure of $(\eta^5\text{-}C_5H_5)_2Rh_2Pd(\mu_3\text{-}CO)(\mu\text{-}\eta^1{:}\eta^2{:}\eta^2\text{-}CF_3C_2CF_3)\{\eta^2\text{-}Ph_2P(CH_2)_2PPh_2\}$ (**III**); the cyclopentadienyl and phenyl rings are omitted for clarity. The atom C(23) is mentioned in the text—this is the phenyl carbon attached directly to C(18).

There are relatively few trinuclear alkyne complexes with an open arrangement of the metals. The structure of $Pt_2Os(CO)_5(PPh_3)_2(\mu_3\text{-}\eta^1{:}\eta^1{:}\eta^2\text{-}MeC_2Me)$ is a rare example reported by Farrugia et al. [32]. More recently, we described the structure of $(\eta\text{-}C_5H_5)_2Rh_2Ir(\mu\text{-}PPh_2)(CO)_2(\mu\text{-}\eta^1{:}\eta^1{:}\eta^2\text{-}CF_3C_2CF_3)$ [20] which has a 48-electron count and a parallel attachment of the alkyne. Thus this conforms to 'normal' behavior for closed clusters. The present complex $(\eta^5\text{-}C_5H_5)_2Rh_2Pd(\mu\text{-}CO)(\mu\text{-}\eta^1{:}\eta^2{:}\eta^2\text{-}CF_3C_2CF_3)\{\eta^2\text{-}Ph_2P(CH_2)_2PPh_2\}$ also has a 48-electron count, but the alkyne lies normal to the non-bonding Rh···Pd axis. This confirms our earlier view that the orientation of the alkyne in cluster and related complexes is critically dependent on the electron density at the metal sites which is influenced by the nature of the attached ligands.

3.4. The solution behavior of $(\eta^5\text{-}C_5H_5)_2Rh_2Pd(\mu_3\text{-}CO)(\mu\text{-}\eta^1{:}\eta^2{:}\eta^2\text{-}CF_3C_2CF_3)\{\eta^2\text{-}Ph_2P(CH_2)_2PPh_2\}$

IR spectra and variable temperature multinuclear NMR spectra indicate that two isomers of the complex co-exist in solution, and that both are fluxional at r.t. The spectra indicate that the major isomer has the structure (**III**) established by X-ray crystallography for the complex in the solid state. The spectroscopic results are consistent with formulation of the minor isomer as $(\eta^5\text{-}C_5H_5)_2Rh_2Pd\{\mu\text{-}\eta^1{:}\eta^2{:}\eta^2C(O)C(CF_3)C(CF_3)\}\{\eta^2\text{-}Ph_2P(CH_2)_2PPh_2\}$ (**IV**). The proportion of the two isomers varies with the solvent (see Table 1) e.g. at 300 K the ratio of (**III**):(**IV**) is about 12.4:1 in chloroform but near 2.5:1 in acetone.

Variable temperature ^{1}H- and ^{19}F-NMR spectra have been recorded for solutions in toluene-d_8, acetone-d_6 and deuterated chloroform. In the ^{1}H spectra at 190 K, two sharp singlets are evident for each of the isomers. As the temperature is raised, all singlets broaden and then the relevant pairs coalesce; eventually, a singlet emerges for each of the isomers. In all solvents, the coalescence temperature (T_c) is near 230 K for (**III**) but close to 270 K for (**IV**).

The profiles for the ^{19}F spectra are somewhat more complex. The most extensive study was done with solutions in toluene-d_8 and these spectra are shown in Fig. 2. At low temperature (209 K), four CF_3 resonances are observed. Two are broadly spaced and are of low relative intensity; these are assigned to isomer (**IV**). The chemical shifts at δ 47.8 and 52.6 are similar to those reported for other complexes incorporating a coordinated $-C(CF_3)=C(CF_3)-C(=O)-$ unit [33]. As the temperature is raised, the relative intensities of these peaks decreases and at 300 K they are no longer detectable. The other resonances are observed near δ 49 and at

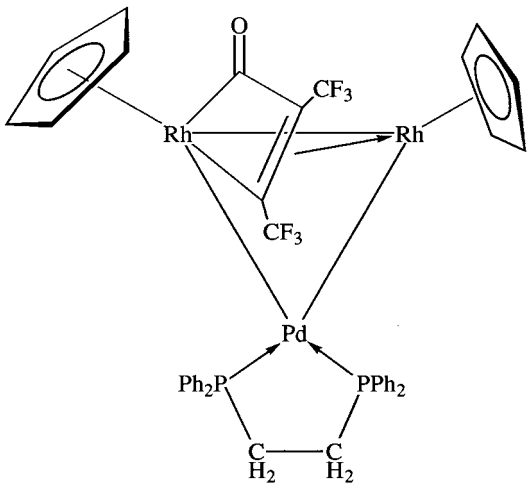

(**IV**)

200 K consist of a broad hump partially overlapping a poorly resolved signal. On raising the temperature, these signals merge and sharpen into a single resonance at δ 48.8. This resonance still has some fine structure. We assign this portion of the spectrum to isomer (**III**) and attribute the unusual profile to restricted rotation of one of the two CF_3 groups.

Further inspection of the molecular structure of (**III**) established that the F(4)···C(23) and F(4)···P(1) non-bonding distances are 3.00 and 3.20 Å, respectively. Molecular modeling [4] then revealed that a counter-clockwise rotation of the CF_3 group containing F(4) by 57.5° about C(4)–C(5) brings F(4) to 2.34 Å from C(23) and 2.73 Å from P(1). This is within the van der Waals contact distances for these atoms and justifies the claim that there is restricted rotation for this CF_3 group.

The $^{31}P\{^1H\}$ spectra for solutions in toluene-d_8 have also been recorded at several temperatures. At 200 K, there are two signals for each of (**III**) and (**IV**), with the resonances for (**III**) being of much higher intensity. As the temperature is increased, the resonances for (**III**) broaden and at 250 K they coalesce; further increase in

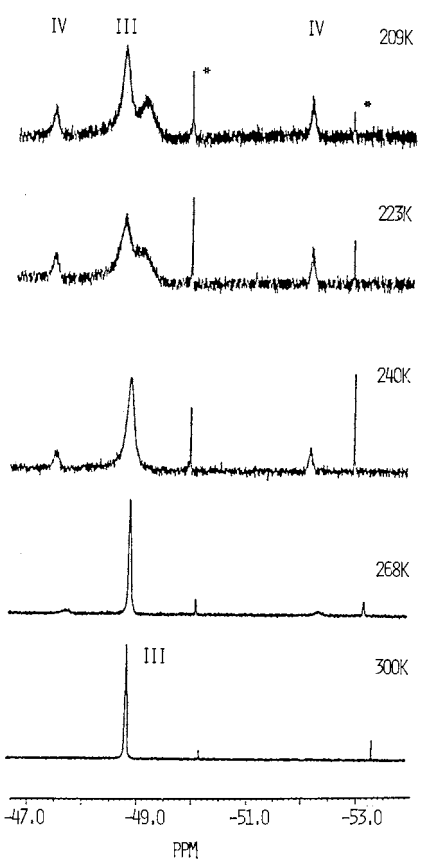

Fig. 2. Variable temperature ^{19}F-NMR spectra for solutions of (**III**)/(**IV**) in toluene-d_8 (* impurity).

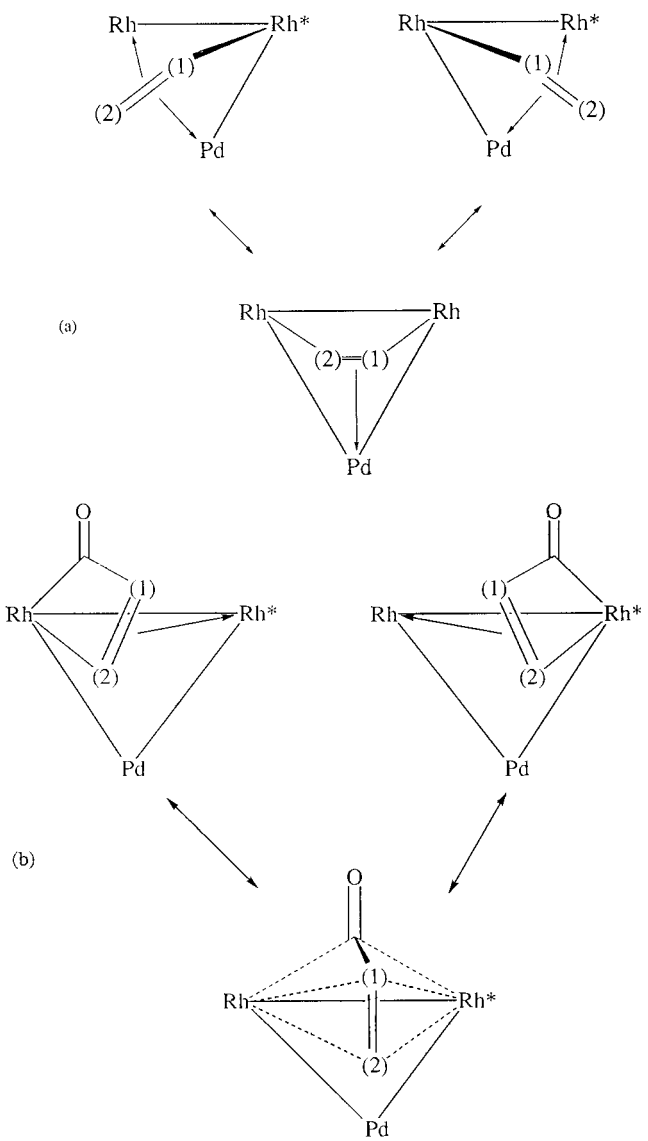

Fig. 3. Pathways for intramolecular rearrangements of (a) (η^5-$C_5H_5)_2Rh_2Pd(\mu_3$-CO)(μ-η^1:η^2:η^2-$CF_3C_2CF_3$){η^2-$Ph_2P(CH_2)_2PPh_2$} (**III**), and (b) (η^5-$C_5H_5)_2Rh_2Pd\{\mu$-η^1:η^2:η^2-C(O)C(CF_3)C(CF_3)}{η^2-$Ph_2P(CH_2)_2PPh_2$} (**IV**). (1) and (2) represent the alkyne carbons and all 'spectator' ligands are omitted for clarity.

temperature results in emergence of a sharp singlet at δ 39.8. The resonances for (**IV**) are essentially unchanged throughout this temperature range.

The rearrangements depicted in Fig. 3 are consistent with all the variable temperature NMR data. In particular, they establish that the cyclopentadienyl groups attached to rhodium atoms become equivalent on the NMR time scale in both (**III**) and (**IV**), that the CF_3 groups become equivalent in (**III**) but not in (**IV**), and that the P atoms attached to palladium become equivalent in (**III**) but not in (**IV**).

4. Summary

A new hetero-trinuclear complex has been structurally characterized. In solution, two isomers co-exist one of which has an open and the other a closed Rh_2Pd core. The crystal and molecular structure of the isomer (**III**), which has the open Rh_2Pd core, reveals an unusual attachment of the alkyne to the metals. The alkyne is σ-bound to the central rhodium and sits across the open Rh···Pd edge. The fluxional behavior of this isomer in solution is best explained by a facile Rh–Pd bond making and breaking process accompanied by a re-orientation of the alkyne. The second isomer (**IV**) has only been identified in solution. It incorporates an acyl group $-C(O)C(CF_3)=C(CF_3)-$ chelated to one of the rhodium atoms in the closed Rh_2Pd core. The attachment of this acyl shifts readily from one rhodium atom to the other. The structure of (**III**) is a significant addition to the array of interesting structures already determined for trinuclear alkyne complexes.

5. Supplementary material available

Tables of fractional atomic coordinates, anisotropic thermal parameters, hydrogen atom parameters, complete bond lengths and angles and observed and calculated structure factors are available as supplementary material.

Acknowledgements

This project has been supported by funds from the ARC small grants scheme. We thank the Australian Government for an Australian Postgraduate Award (to G.R. County). Brian Mann (University of Sheffield) provided helpful comments on the NMR spectra that increased our understanding of these systems.

References

[1] See references in Comprehensive Organometallic Chemistry II, in: E.W. Abel, F.G.A. Stone, G. Wilkinson, (Eds.), Heteronuclear Metal–Metal Bonds, vol. 10, (R. Adams, vol. Ed.), Elsevier, Amsterdam, 1995.
[2] J.-F. Hallet, Coord. Chem. Rev 143 (1995) 637.
[3] R.S. Dickson, G.D. Fallon, K.D. Heazle, M.J. Liddel, J. Organomet. Chem. 430 (1992) 221.
[4] InsightII, MSI, San Diego, CA.
[5] W.F.L. Amerego, D.D. Perrin, D.R. Perrin, Purification of Laboratory Chemicals, 2nd ed., Pergamon, Oxford, 1980.
[6] R.S. Dickson, S.H. Johnson, G.N. Pain, Organomet. Synth. 4 (1988) 283.
[7] G.R. County, R.S. Dickson, G.D. Fallon, S.M. Jenkins, J. Johnson, J. Organomet. Chem. 296 (1996) 279.
[8] Y. Tatsuno, T. Yoshida, S. Otsuka, Inorg. Synth. 19 (1979) 220.
[9] G.M. Sheldrick, SHELXTL Plus, Revision 3.4, Siemens Analytical X-ray Instruments, 1988.
[10] G.R. County, R.S. Dickson, S.M. Jenkins, J. Johnson, O. Paravagna, J. Organomet. Chem. 530 (1997) 49.
[11] B.L. Shaw, Proc. Chem. Soc. (1960) 247.
[12] S. Otsuka, T. Yoshida, M. Matsumoto, K. Nakatsu, J. Am. Chem. Soc. 98 (1976) 5850.
[13] P. Leoni, M. Pasquali, T. Beringhelli, G. D'Alfonso, A.P. Minoja, J. Organomet. Chem. 488 (1995) 39.
[14] T. Yoshida, S. Otsuka, Inorg. Synth. 28 (1990) 113.
[15] S. Lo Schiavo, E. Rotondo, G. Bruno, F. Faraone, Organometallics 10 (1991) 1613.
[16] C.G. Arena, E. Rotondo, F. Faraone, M. Lanfranchi, A. Tiripicchio, Organometallics 10 (1991) 3877.
[17] J.P. Farr, M.M. Olmstead, A.L. Balch, J. Am. Chem. Soc. 102 (1980) 6654.
[18] A.L. Balch, L.A. Fossett, M.M. Olmstead, D.E. Oram, P.E. Reedy Jr., J. Am. Chem. Soc. 107 (1985) 5272.
[19] R.S. Dickson, O.M. Paravagna, Organometallics 10 (1991) 721.
[20] R.S. Dickson, O.M. Paravagna, Organometallics 11 (1992) 3196.
[21] E.R. Corey, L.F. Dahl, W Beck, J. Am. Chem. Soc. 85 (1963) 1202.
[22] O.S. Mills, E.F. Paulus, J. Organomet. Chem. 10 (1976) 331.
[23] P. Braunstein, C. de Méric de Bellefon, M. Ries, J. Fischer, S.-E. Bouaoud, D. Grandjean, Inorg. Chem. 27 (1988) 1327.
[24] J. Chatt, J., P.B. Hitchcock, A. Pidock, C.P. Warrens, K.R. Dixon, J. Chem. Soc. Dalton Trans. (1984) 2237.
[25] J. Chatt, P.B. Hitchcock, A. Pidcock, C.P. Warrens, K.R. Dixon, J. Chem. Soc. Chem. Commun. (1982) 932.
[26] A.J. Carty, N.J. Taylor, E. Sappa, Organometallics 7 (1988) 405.
[27] J.F. Blount, L.F. Dahl, C. Hoogzand, W. Hübel, J. Am. Chem. Soc. 88 (1966) 292.
[28] S. Rivomanana, G. Lavigne, N. Lugan, J.-J. Bonnet, Organometallics 10 (1991) 2285.
[29] A.J.P. Domingos, B.F.G. Johnson, J. Lewis, J. Organomet. Chem. 36 (1972) C43.
[30] A.J. Deeming, S. Hasso, M. Underhill, J. Chem. Soc. Dalton Trans. (1975) 1614.
[31] M. Tachikawa, J.R. Shapley, C.G. Pierpont, J. Am. Chem. Soc. 97 (1975) 7172.
[32] L.J. Farrugia, J.A.K. Howard, P. Mitrprachachon, F.G.A. Stone, P. Woodward, J. Chem. Soc. Dalton Trans. (1981) 162.
[33] R.S. Dickson, G.S. Evans, G.D. Fallon, Aust. J. Chem. 38 (1985) 273.